A validated design simulation tool for passive solar space heating: Results from a monitored house in West Lothian, Scotland

A. Girard, T. Muneer and G. Caceres

Indoor and Built Environment 2014 23: 353 originally published online 26 April 2013
DOI: 10.1177/1420326X13480057

Original Paper

Indoor and Built Environment

Indoor and Built Environment
2014, Vol. 23(3) 353–372

DOI: 10.1177/1420326X13480057
ibe.sagepub.com

SAGE

A validated design simulation tool for passive solar space heating: Results from a monitored house in West Lothian, Scotland

A. Girard[1], T. Muneer[2] and G. Caceres[3]

Abstract

Determining the availability of renewable sources on a particular site would result in increasing the efficiency of buildings through appropriate design. The overall aim of the project is to develop a pioneering software tool allowing the assessment of possible energy sources for any building design project. The package would allow the user to simulate the efficiency of the Passive Solar Space Heating referred in the Low and Zero Carbon Energy Sources (LZCES) Strategic Guide stated by the Office of the Deputy Prime Minister (2006) and the Building Regulations. This research paper presents the tool for modelling the passive solar sources availability in relation to low-carbon building. A 3-month experimental set up monitoring a solar house in West Lothian, Scotland, was also undertaken to validate the simulation tool. Experimental and simulation results were found in good agreement following a one-to-one relationship demonstrating the ability of the newly developed tool to assess potential solar gain available for buildings. This modelling tool is highly valuable in consideration of the part L of the Building Regulations (updated in 2010).

Keywords

Building design, Combination selection, Efficiency, Renewable energy, Simulation, Solar air heater

Date received: 13 September 2012; accepted: 2 February 2013

Introduction – Method aiming at estimating the solar energy to harness

Increase in green house gases concentrations is directly responsible for the rise in the average temperature of Earth's atmosphere (global warming). Reports by the Inter-governmental Panel on Climate Change (IPCC) have raised public awareness of energy use and the climate change implications.[1] It was estimated that in 2002 buildings worldwide accounted for about 33% of the global greenhouse gas emissions.[2] Energy efficiency and carbon emissions have recently started to have significant influence on the evolution of the construction industry. The industry is experiencing a strong push towards the improvement of the energy performance of new and refurbished buildings, driven by the need to reduce carbon dioxide emissions. Much work has been carried out in this area, including 40% House Project and the approved document L1A on New Dwellings (2010 of the Building Regulations).[3] However, government has recently signalled its intention to initiate a radical improvement in the energy efficiency requirements for new and refurbished buildings in 2010 and beyond.[3–6] It is intended that all new dwellings will need to be built as ''zero net carbon emissions'' by 2016 and all non-dwellings by 2019.[7,8] There is a broad spectrum of energy saving technologies and design approaches that are currently available to at

[1]Faculty of Engineering and Sciences, University Adolfo Ibañez, Altos del Sporting. Viña del Mar, Chile
[2]School of Engineering and Built Environment, Edinburgh Napier University, Edinburgh EH10 5DT, UK
[3]Faculty of Engineering and Sciences, University Adolfo Ibañez, Peñalolén, Santiago, Chile

Corresponding author:
A. Girard, Faculty of Engineering and Sciences, University Adolfo Ibañez, Av. Padre Hurtado 750, Altos del Sporting. Viña del Mar, Chile.
Email: aymeric.girard@gmail.com

least partially meet the above futuristic regulations. At one extreme, a building could meet the proposed requirement if it generated sufficient energy to offset its fossil fuel consumption.[9] At the other end, the building could be of a radically different type of construction requiring no fossil fuel. There is a conceptual understanding of a Zero Energy Building as an energy efficient building able to generate electricity, or other energy carriers, from renewable sources in order to compensate for its energy demand.[7] Chesné et al. have pointed out a method for designing zero net carbon emissions buildings, which consists of assessing both the capacity of the resources (sun, sky and outside air) to cover the building needs, and the ability of the building to exploit the available energy resources.[10]

The building services engineering in every sector (transport, defence, process, healthcare etc) is seeking the adequate solution to bring the provision of Low and Zero Carbon Energy Sources (LZCES)[11] in projects and generate the electrical and thermal energy for candidate buildings. The building services design professionals are using many software tools in order to model and estimate their building energy demand and carbon footprint. These tools are somewhat lacking on the simulation of renewable energy features design. The work consists in the assessment of a solar space heating experiment in East Whitburn, daylight measurement, numerical analysis, graphical analysis; simulation work aims at defining a new innovative tool using a building thermal model to determine the on-site solar passive energy available in UK conditions. It can be considered as a decision-making tool concept for building services engineers.

Passive solar space heating simulation

The analysis looks at the amount of solar energy available to harness via Passive Solar Space Heating (PSSH) design. The PSSH Model can be used UK-wide to easily evaluate the energy production (or savings), life-cycle costs and greenhouse gas emissions reduction. The building geometry and the 14 Chartered Institution of Building Services Engineers (CIBSE) weather[12] stations data on solar irradiance and external temperature are used to model PSSH.

To design a building that would maximise space heating through passive solar energy source, it is intended that the building envelope acts as the primary climate modifier in order to reduce energy demand with the services trimming the conditions to suit the occupant requirements. The analysis of the building envelope is the most important as it enables the architectural design and the material to be selected accordingly.

A good envelope design that integrates with the building services helps to reduce the energy demand and minimise the need for services. A number of options to make use of PSSH are available and these would be beneficial to the users. A careful analysis of the potential impacts of the orientation, the wall versus window ratio, the air tightness and the thermal insulation would need to be taken into consideration.

This part enables assessment of the impact of the design and the on-site LZCER on the indoor temperature conditions. It describes the use of data such as location, external wall, size, areas, area of glazing, windows, building's type along with the external temperature, solar gains, U values from CIBSE.[13] The use of the above data placed into a thermal network enables the sub-hourly temperature calculation of a building's electrical demand, water consumption, heating and cooling demand.

Description of the PSSH experiment

This section aims to explain the experiment concerning the solar house monitoring in East Whitburn. It details the test set up, measurement, data collection and draws conclusions on summer and winter conditions.

The amount of energy available from the sun outside the Earth's atmosphere is approximately 1,361 $W\,m^{-2}$.[14] This is known as the solar constant. Absorption occurs whilst the solar radiation passes through the atmosphere, which on clear days results in solar energy available at the Earth's surface in the direction of the sun to be in the region of 1,000 $W\,m^{-2}$. This energy radiated to the earth undergoes monthly and diurnal variations. The total radiation from the sun will have beam and diffuse components. The earth's atmosphere and cloud cover will determine the extent of diffusion, thus influencing solar radiation availability.

Pyranometers allow for the accurate measurement of diffuse and global (diffuse and beam) radiation on horizontal surfaces. By using global and diffuse radiation data, it is possible to calculate the energy incident on tilted surfaces. The solar energy incident is dependent on the orientation of a surface and the time of year. It is proven that at midday of the spring and autumn equinox a surface tilted at an angle equal to its latitude is perpendicular to the sun's rays.[15] Duffie and Beckman[16] suggested the optimum angle of tilt of a surface to be 0.9 times the latitude of the location. For Edinburgh where the latitude is 56° the optimal angle would be 50.4°.

Solar energy using RE availability maps

The solar radiation can be directly measured on-site by the use of a pyranometer. If data collection is not

possible, solar data can be collected directly from the British Atmospheric Data Centre (BADC) or the CIBSE/Met Office Hourly Weather Data for 14 locations across the UK. Thereafter, an estimation of the irradiation can be performed using solar geometry depending on the site location.

Solar geometry simulation

Solar radiation availability on a tilted surface can be calculated using horizontal irradiance data by means of a model developed by Muneer.[15,17] A calculation of the solar incident on a sloping surface is possible using the angle of INCidence (INC), SOLar ALTitude (SOLALT), SOLar AZiMuth (SOLAZM), Wall AZimuth (WAZ) and the TiLT of the surface (TLT). The co-ordinates that depict the sun's position in the sky are dependent upon apparent solar time, the solar declination and the latitude and longitude of the location.

The angle of INCidence (INC) is calculated using equation (1), where the Wall AZimuth (WAZ) is positive in a clockwise direction from north on a horizontal plane.

$$\cos \mathrm{INC} = \cos \mathrm{SOLALT}.\cos(\mathrm{SOLAZM} \pm \mathrm{WAZ}).\sin \mathrm{TLT} + \cos \mathrm{TLT}.\sin \mathrm{SOLALT} \quad (1)$$

The SOlar ALTitude (SOLALT) and SOlar AZiMuth (SOLAZM) can be calculated using the LATitude coordinate (LAT), solar DEClination (DEC) and Solar Hour Angle (SHA) as in equations (2) and (3) as follows.

$$\sin SOLALT = \sin LAT.\sin DEC - \cos LAT.\cos DEC.\ \cos SHA \quad (2)$$

$$\cos SOLAZM = \frac{\cos DEC \times (\cos LAT.\tan DEC + \sin LAT.\cos SHA)}{\cos SOLALT} \quad (3)$$

The solar hour angle is the position of the sun in relation to the local meridian at 15° per h. The solar declination (DEC) is the angle of the earth-sun vector calculated by using equation (4), where the day number (DN) equals one for January the first and is the total number of days gone by so far in any selected year.[18]

$$\mathrm{DEC} = \sin^{-1}\{0.39795 \times \cos[0.98563 \times (\mathrm{DN} - 1)]\} \quad (4)$$

Apparent Solar Time (AST), determined from equation (5), is required for solar geometry equations to correct the difference between the time for a specified locality at a certain LONGitude (LONG) and the Standard time Meridian (LSM). For locations east of LSM, the longitudinal correction term in the square brackets is positive.

$$AST = standard\ time\ (local\ civil\ time) + EOT \pm \frac{LSM - LONG}{15} \quad (5)$$

The equation of time (EOT) relates to the difference between the standard time recorded by clocks running at normal speed and solar time. EOT is calculated using equation (6) as follows:[17,18]

$$\mathrm{EOT} = 0.1236 \sin x - 0.0043 \cos x + 0.1538 \sin 2x + 0.0608 \cos 2x \quad (6)$$

where

$$x = \frac{360 \times (DN - 1)}{365.242} \quad (7)$$

The Slope Irradiation (SIr), equation (8), is required to estimate the amount of solar energy on a surface.

$$SIr = BSRAD + DSRAD + GR \quad (8)$$

Beam Solar RADiation (BSRAD) can be calculated from equation (9):

$$BSRAD = (GRAD - DRAD) \times \frac{\cos(INC \times DTOR)}{\sin(SOLALT \times DTOR)} \quad (9)$$

Diffuse Solar RADiation (DSRAD) is determined by equation (10):

$$\mathrm{DSRAD} = \mathrm{DRAD} \times \cos\left(\mathrm{TLT} \times \frac{\mathrm{DTOR}}{2}\right)^2 \times \left(1 + \mathrm{CLRFRA} \times \sin\left(\mathrm{TLT} \times \tfrac{\mathrm{DTOR}}{2}\right)^3\right) \times \begin{pmatrix} 1 + \mathrm{CLRFRA} \\ \times\cos[(\mathrm{SOLINC} \times \mathrm{DTOR})^2] \\ \times\cos[(\mathrm{SOLALT} \times \mathrm{DTOR})^3] \end{pmatrix} \quad (10)$$

CLeaR FRAction (CLRFRA) is defined by equation (11):

$$\mathrm{CLRFRA} = \frac{(\mathrm{GRAD} - \mathrm{DRAD})}{\mathrm{ERAD}} \quad (11)$$

Calculate horizontal Extraterrestrial irRADiance (ERAD) using equation (12):

$$\mathrm{ERAD} = 1361 \times (1 + 0.033 \times \cos(0.0172024 \times d)) \times \sin(\mathrm{SOLALT} \times \mathrm{DTOR}) \quad (12)$$

The conversion of Degree TO Radian (DTOR) is given by equation (13) as:

$$DTOR = \frac{\pi}{180} \quad (13)$$

The Ground Reflect (GR) can be found using the equation (14) where ρ is the reflective angle

$$\mathrm{GR} = \rho \times \mathrm{GRAD} \times \sin\left(0.5 \times \mathrm{TLT} \times \frac{\pi}{180}\right)^2 \quad (14)$$

All these equations are included in the PSSH simulation tool. PSSH provides a generic mechanism for

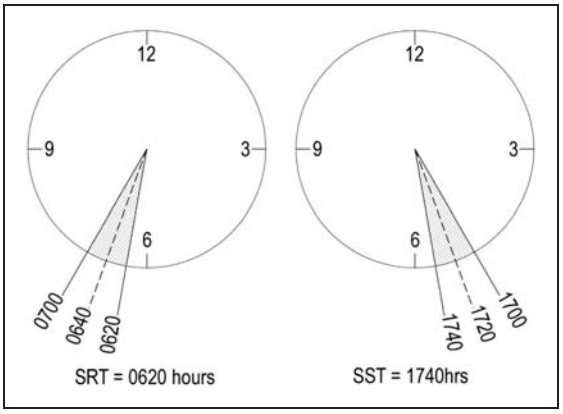

Figure 1. Correction for first and final partial hours of daylight. Where true Sunrise time (SRT) is 0620, for example, the solar geometry at 0640 is used in calculations of energy and irradiation since this is the midpoint between SRT and the start of the next hour. An equivalent correction is used for sunset time (SST).[19]

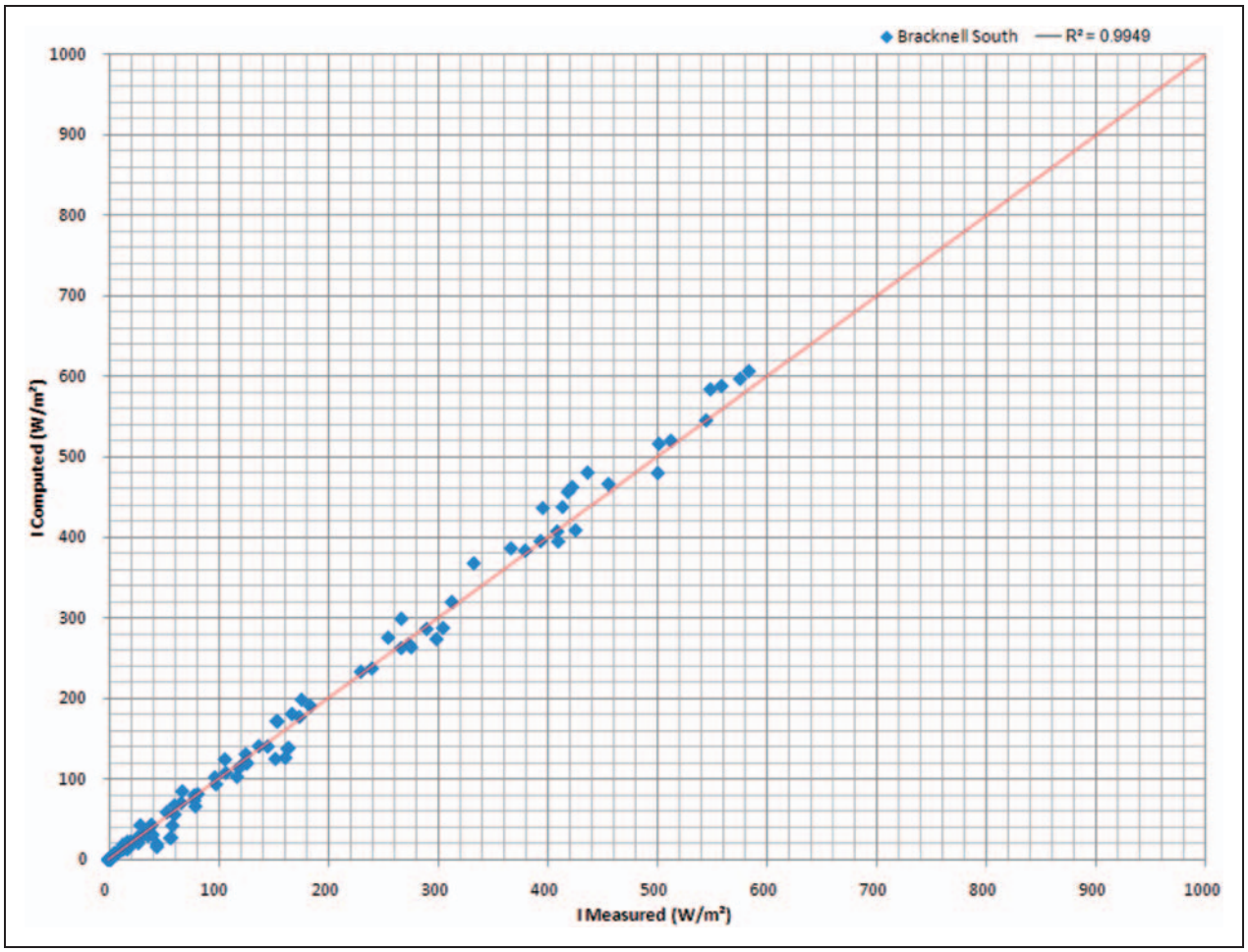

Figure 2. Hourly computed vs experimental slope irradiance for Bracknell South aspect.

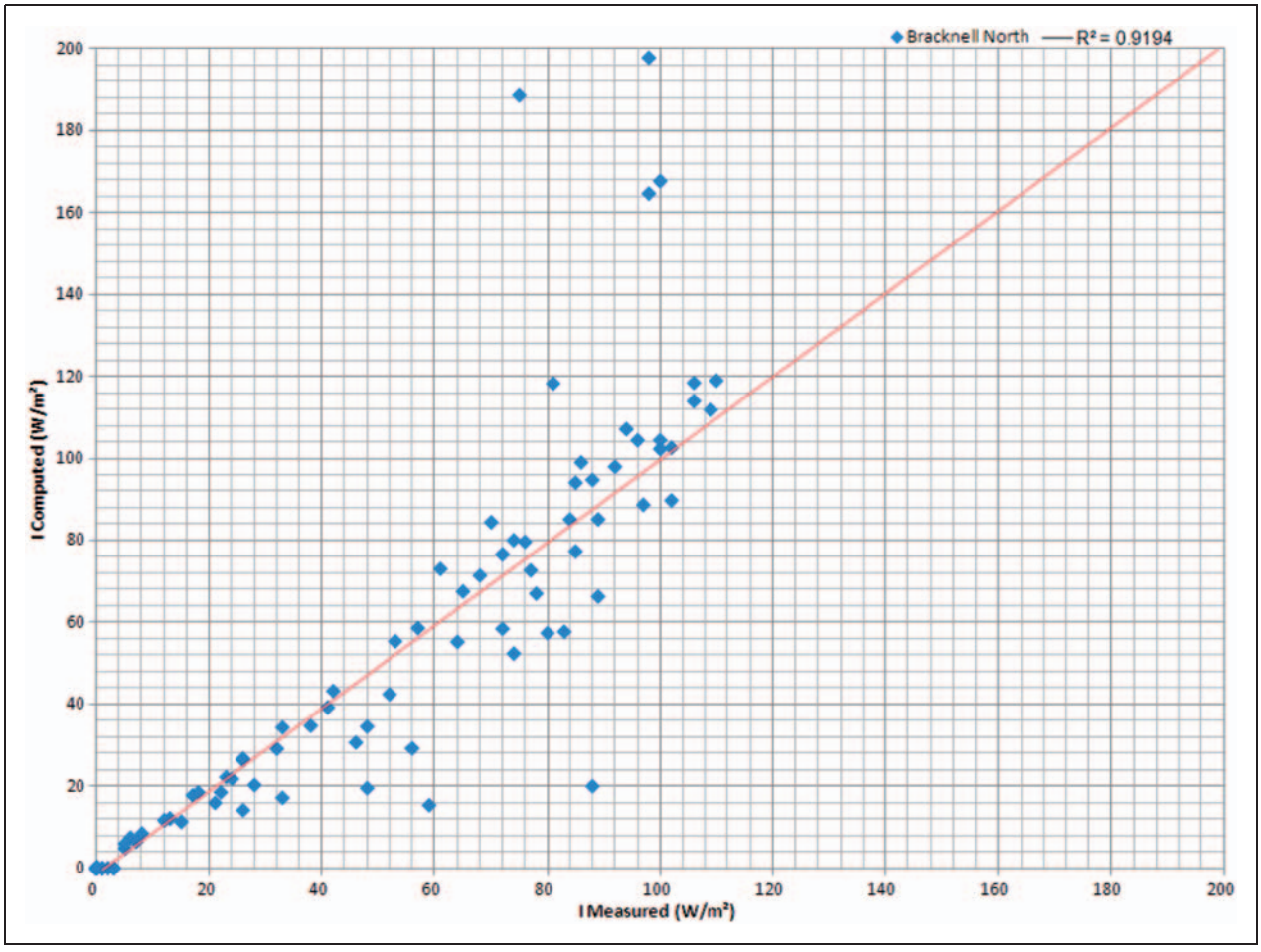

Figure 3. Hourly computed vs experimental slope Irradiance for Bracknell North aspect.

managing input data sets via a specific worksheet. The simulation can be duplicated and renamed as many times as required using the standard Microsoft Excel interface. It provides a basic data cleaning function to check for anomalous values. The current support for process structure in the Microsoft Visual Basic for Applications (VBA) code, however, relies mainly on the adaptation of the examples supplied.

PSSH is a tool for calculating both incident energy and illuminance on an arbitrarily oriented surface for any location in the world based on parameters supplied by the user. It combines the established algorithms with an innovative correction factor for the first and final partial hours of daylight, which involves using the solar geometry at the midpoint of those periods,[19] see Figure 1. Using hourly global and diffuse irradiation data for the Bracknell location, slope irradiation was plotted to compare the measured versus computed data over 4 days on a vertical plane, as shown in Figures 2 to 5. The Irradiance (I) is expressed in $W\,m^{-2}$.

Using sub-hourly global and diffuse irradiation data for the Edinburgh location, slope irradiation was plotted to compare the measured versus computed data over 1 month on a vertical plane, as shown in Figures 6 to 9.

Computed data versus experimental data were plotted on a scatter graph in Figures 2 to 9 to examine the validity of the simulation. It was demonstrated that the experimental and computed simulation results are strongly correlated as they follow a 1:1 relationship. North aspects plots for Bracknell and Edinburgh as shown in Figure 3 and 8 reveal lower values due to less irradiation.

Field experiment: Temperature monitoring

The objective of the experiment is to plot the efficiency of the solar house, which is the ratio of the useful heat gain over a particular time period to

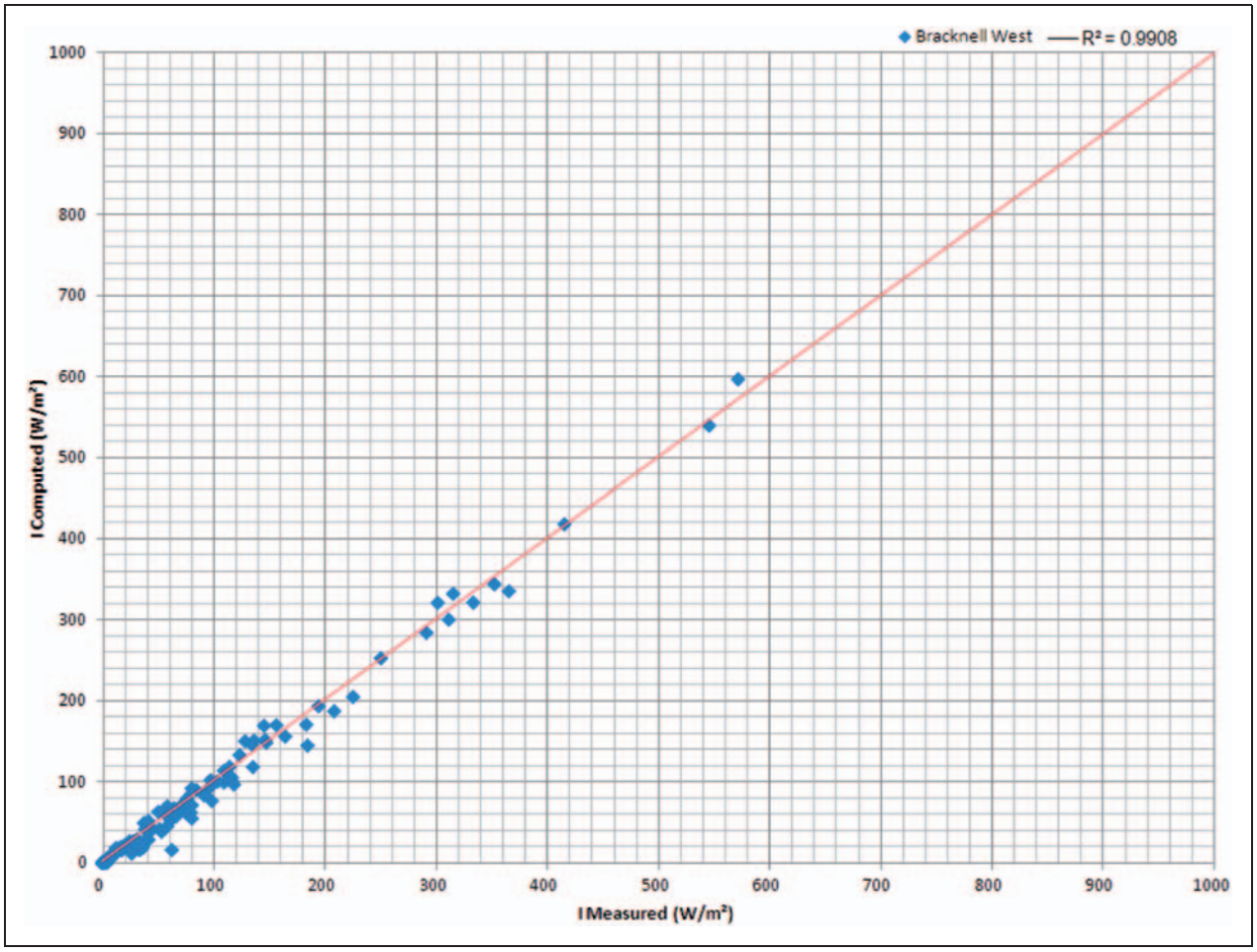

Figure 4. Hourly computed vs experimental slope irradiance for Bracknell West aspect.

the cumulative incident energy over the same time period.

Experimental tests were carried out on the solar house. It is shown in Figure 10 that the solar house is constructed using conventional structural insulated panels (SIPs) in order to minimise heat losses in a northern latitude location. By means of a data logger, eight K-type thermocouples were used to monitor the indoor air temperature rise over 10-min intervals for summer (May–June) and winter (December–January) conditions.

Figure 11 indicates the location of the two pyranometers and the ten thermocouples at different heights within the house. Each thermocouple was calibrated using melting ice for the 0°C and the steam of distilled boiling water for 100°C. The tolerance is ±0.5°C. A control volume approach was used to determine a weighted average of the indoor air temperature (Figure 12).

The Southern façade is composed of large double-glazed windows. The U Value of the windows and walls are equal to $3.3\,W\,m^{-2}K$ and $0.4\,W\,m^{-2}K$. The U value represents the overall heat transfer coefficient expressed in ($W\ m^{-2}K$). The opaque elements of the envelope play a role in effective passive solar design. The external walls of the studied building named SIPs have three layers. The three layers are defined as 10 mm of inner Oriented Strand Board (OSB) sheathing, a 100-mm of Styrene Butadiene Styrene (SBS) polyurethane foam core insulation layer and an outer OSB sheathing of 10 mm. Roof is similarly composed.

Field experiment: Daylight monitoring

In May and December 2007, solar radiation data as well as the inner and outer temperatures of a solar house were recorded. Global solar radiation is a major source of energy that varies with time of day and year. The precision measurement of solar radiation is very important for the solar heat gain estimation.

The pyranometer allows measurement of solar radiation on a plane surface. The CM11 pyranometer by Kipp & Zonen^{TM} with sensitivity 4–6 $\mu V/W/m^2$ was used for the experiment. The sensors use an upwards

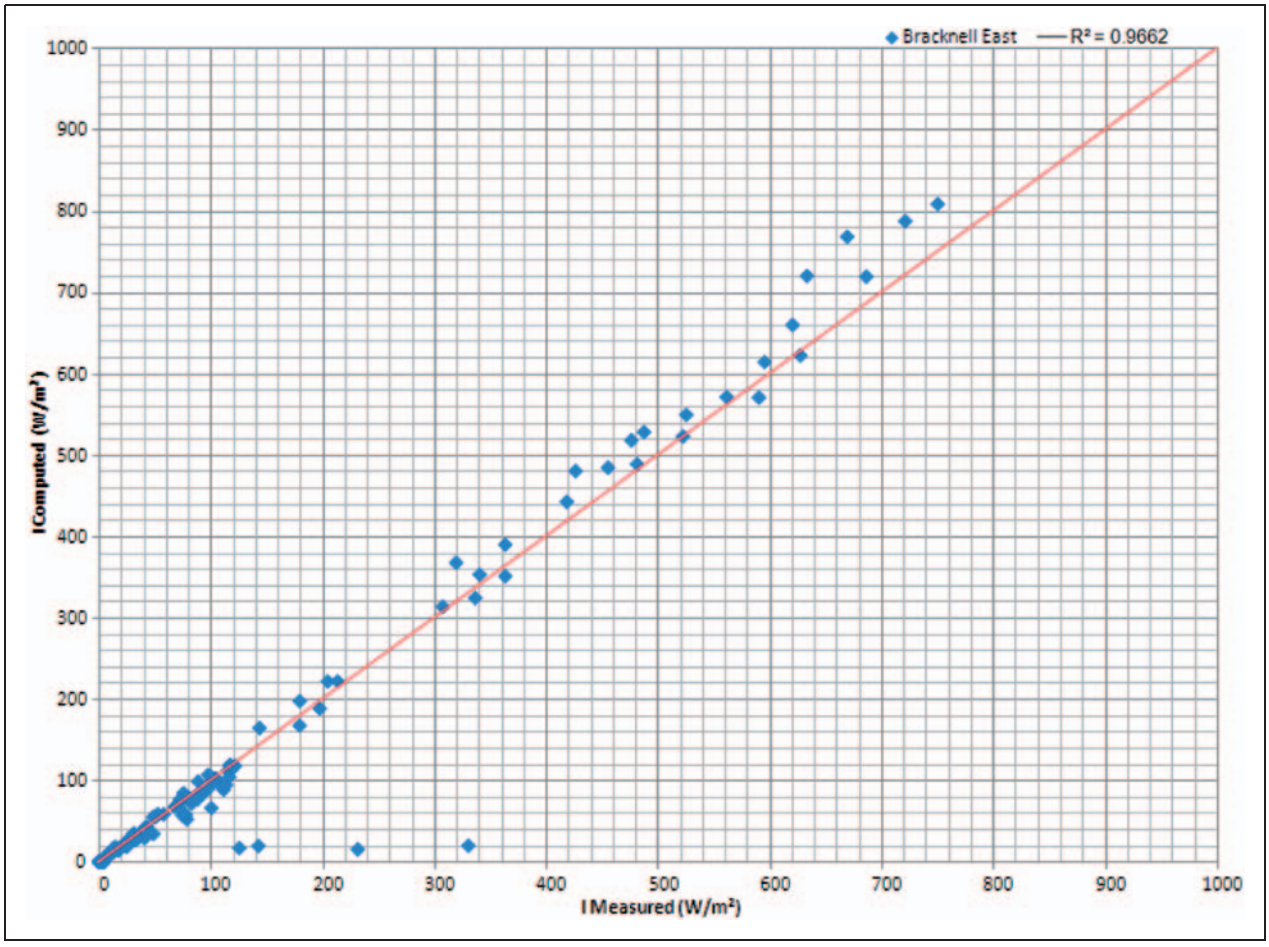

Figure 5. Hourly computed vs experimental slope irradiance for Bracknell East aspect.

facing black disc with a radial heat conduction path for rapid response. The temperature between the discs is a direct function of the intensity of radiation absorbed by the receiver disc. The disc temperature was precisely determined by a thin film platinum resistance element to provide exceptional linearity and stability. The pyranometer used to record sunshine duration or total incident solar radiation was fixed on the solar house's fascia board. The data recorded were received in mV, a factor was used to permit conversion of the data into $W\,m^{-2}$. The solar meter calibration factor was equal to $5.62.10^{-6}\,V/W\,m^2$.

Uncertainties and errors associated with measurements

Equipment error and uncertainty

Temperatures in the house were measured using K-type thermocouples. The uncertainty in thermocouple measurement after calibration was found to be $\pm 0.5^{\circ}C$. Uncertainties associated with calibration were neglected as accurate methods were used to define the temperature of each thermocouple. An additional uncertainty of $0.1^{\circ}C$ was associated with data logger conversion due to its limitation in resolution.

Field experiments equipment used for control and measurements have associated uncertainties. The pyranometer has an estimated uncertainty in global radiation measurement of $\pm 5\,W\,m^{-2}$ at 95% confidence limits. This suggests that 95% of individual readings were within the stated limits under normal climatic conditions.

Operational errors

In addition to the sources of equipment-related errors, care was taken to avoid the following operational-related problems and errors:

- Complete or partial shade of the pyranometer from direct sunlight by buildings
- Dust, snow, dew, water-droplets, bird droppings etc.
- Incorrect sensor levelling
- Processing errors, human errors or calibration errors are amongst others.

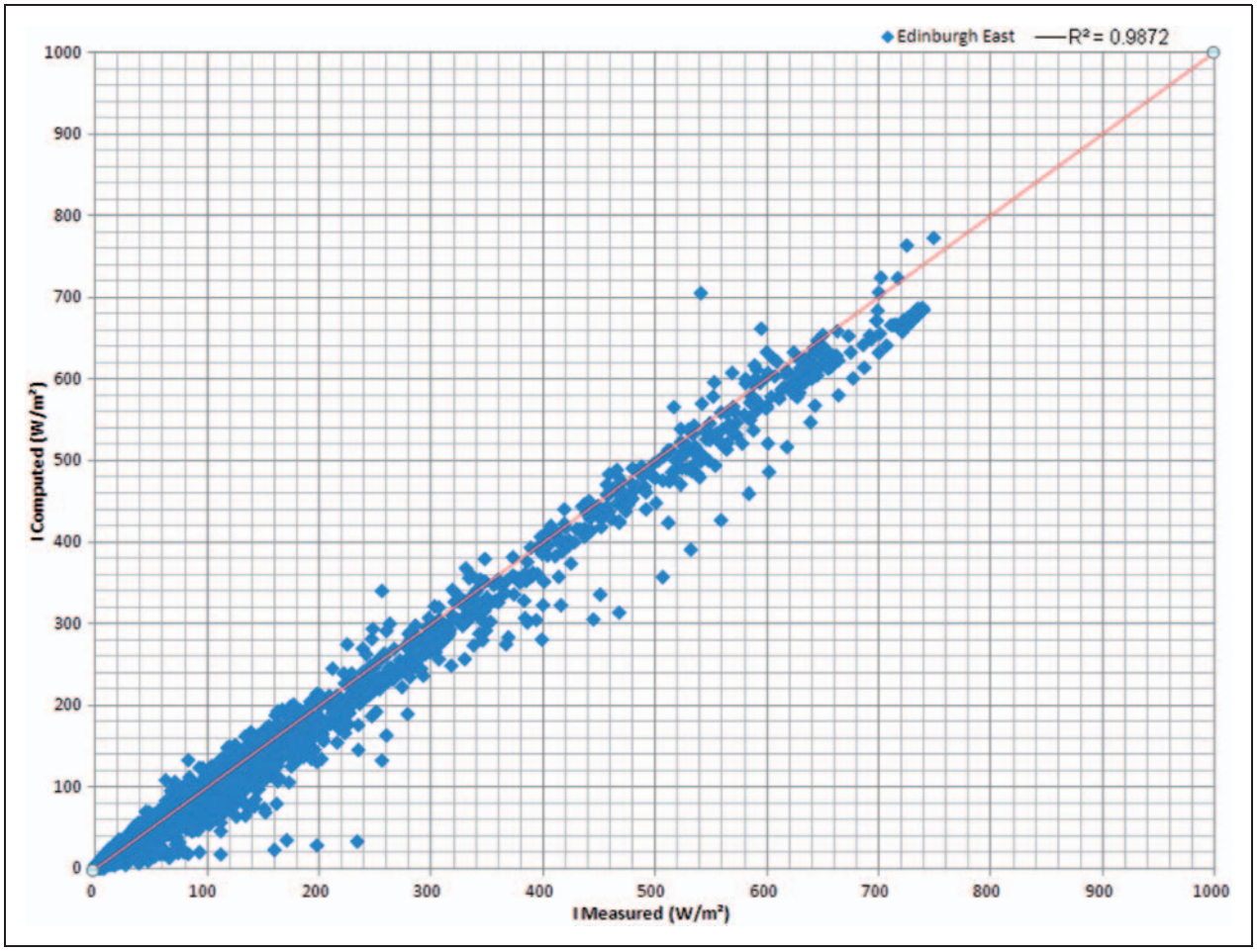

Figure 6. Hourly computed vs experimental slope irradiance for Edinburgh – East aspect.

Building energy benchmarking related to the location

Once gathered, all data were entered into a spreadsheet application to start the analysis. The average of the inner and outer temperatures of the house was labelled as T_i and T_o.

The solar house is located in an isolated area. Its roof is high enough to avoid shadowing and to find optimum solar gains all year round. The solar house is installed with high window areas on its 180° south-facing side which permits to obtain optimum solar gains.

The experimental study covered the time when the building was unoccupied and doors were supposed to be closed. The external characteristic of the external envelope of the house is shown in Table 1, where h represents the convective heat transfer coefficient expressed in ($W\,m^{-2}\,K$). As a first experimental model, the building was assumed to be airtight. Therefore no losses by ventilation were considered. The internal thermal mass of the building was considered with a survey of existing furniture and internal envelope composition. The solar house was considered as one mass.

Internal and external fabric walls surfaces and mass was calculated in order to obtain the best estimation of thermal mass. The thermal values for the different types of windows are taken from Figure 13.

Two measures were taken for summer and winter conditions. Data was collected from the 5th of May to the 7th of June and from the 9th of January to the 7th of February 2008, plotted on a graph in an MS Excel spreadsheet.

Figure 14 shows the profile of the solar energy transmitted with the average of inner and outer temperatures of the house for a selected day. The data plotted in Figure 14 shows that the average temperature inside the solar house followed a similar trend to the amount of solar radiation. The outer temperature of the solar house was also reacting with the solar irradiance but was not as clear as the inside temperature due to external effects.

The solar irradiance is usually optimal when the sun is at the highest solar altitude degree around midday

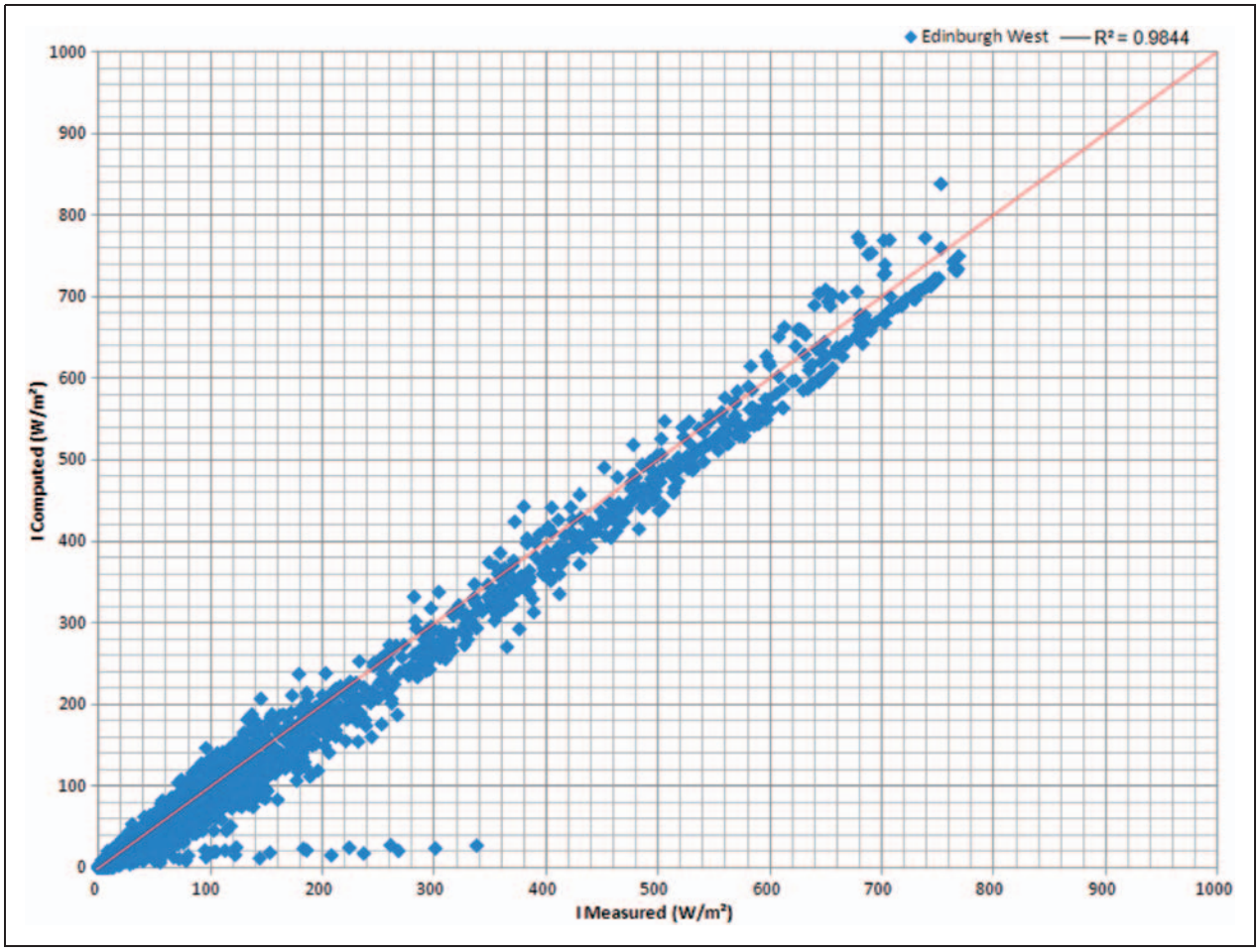

Figure 7. Hourly computed vs experimental slope irradiance for Edinburgh – West aspect.

with a clear sky. Also, its irradiance level allows seeing which day the sky was clear and how the temperature reacts with different weather (cloudy, rainy . . .).

Another important point is to visualise the inner and outer temperature difference rising up to 20°C–25°C even if the temperature is taken from December, which shows the solar house operates with high efficiency. The results tend to confirm the large potential of solar building design to reach significant levels of energy saving in northern latitudes.

Thermal performance and efficiency

The solar house was studied similar to a thermal network called the "Thermal Resistance Network" (TRN). This network allows modelling the energy gains and losses from the solar house. A TRN diagram representing the solar house is shown in Figure 15.

In this diagram, Rconv represents the convective Resistance expressed in (m^2 K/W), Rrad the radiation Resistance in (m^2 K/W), Rcond the conductive Resistance in (m^2 K/W), m the mass of the material in (kg), C_p the thermal Capacitance of the material in (J/kg.K), T_{is} the inner skin Temperature (K), T_i the inside Temperature (K), T_{os} the outer skin Temperature (K), T_o the ambient Temperature (K) and Tsky the sky Temperature (K).

Energy received: Solar gains

The building has a direct solar gain through southern windows on the floor and back walls combined with their mass storage. The solar radiation incident on the glass cover is largely transmitted with only a small fraction absorbed and reflected, see Figure 16 taken from the transmission curve spreadsheet.[20]

This step allows the calculation of the sun energy coming into the house. The light transmission "τ" of the windows needs to be found, the curve and equation of double glazed windows were taken from the excel document using Windows in Buildings.[17] Figure 16 shows the transmission curve and the equation (15) of the light transmission "τ" in relation to the angle of incidence.

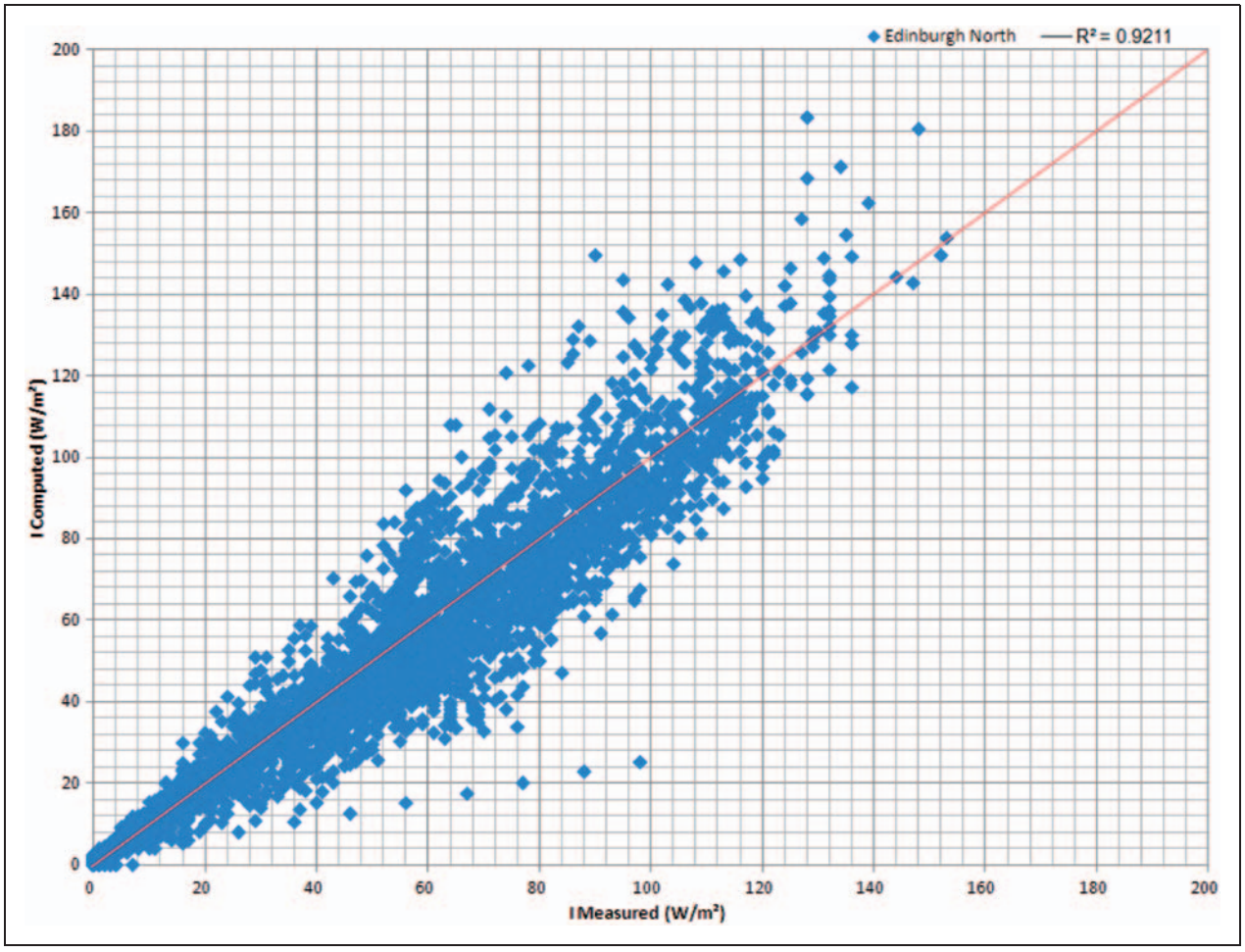

Figure 8. Hourly computed vs experimental slope irradiance for Edinburgh – North aspect.

The Light transmission "τ" was obtained using equation (15) of the transmission curve; the result is shown in Figure 16:

$$\tau = -1e^{-8} \times i^4 - 2e^{-7} \times i^3 + 5e^{-5} \times i^2 - 0.0014 \times i + 0.7058 \quad (15)$$

The energy transmitted was calculated using equations (16) and (17):

$$\text{Energy transmitted}\left(\frac{W}{m^2}\right) = \text{solar radiation}\left(\frac{W}{m^2}\right) \times \text{light transmission } \tau \quad (16)$$

and

$$Q_{in1}(W) = \text{Energy transmitted}\left(\frac{W}{m^2}\right) \times \text{Area windows } (m^2) \quad (17)$$

Q represents the heat transfer rate expressed in Watts (W).

Building numerical analysis

Several meetings with the landlord, surveys and measurement of the building materials were conducted to allow estimation of the building composition, volume and thermal mass.

Figure 17 shows the different dimensions taken from the house to assess the house geometrical analysis. The values were measured on-site and taken from the architectural layout.

Then, the thermal material characteristics are defined as given in equation (18).

$$\text{U Value} = \frac{1}{(R_P + R_G + R_F)} \quad (18)$$

where R_P, R_G, R_F are the thermal resistances of the inner OSB sheathing, SBS polyurethane foam core and outer OSB sheathing calculated from the

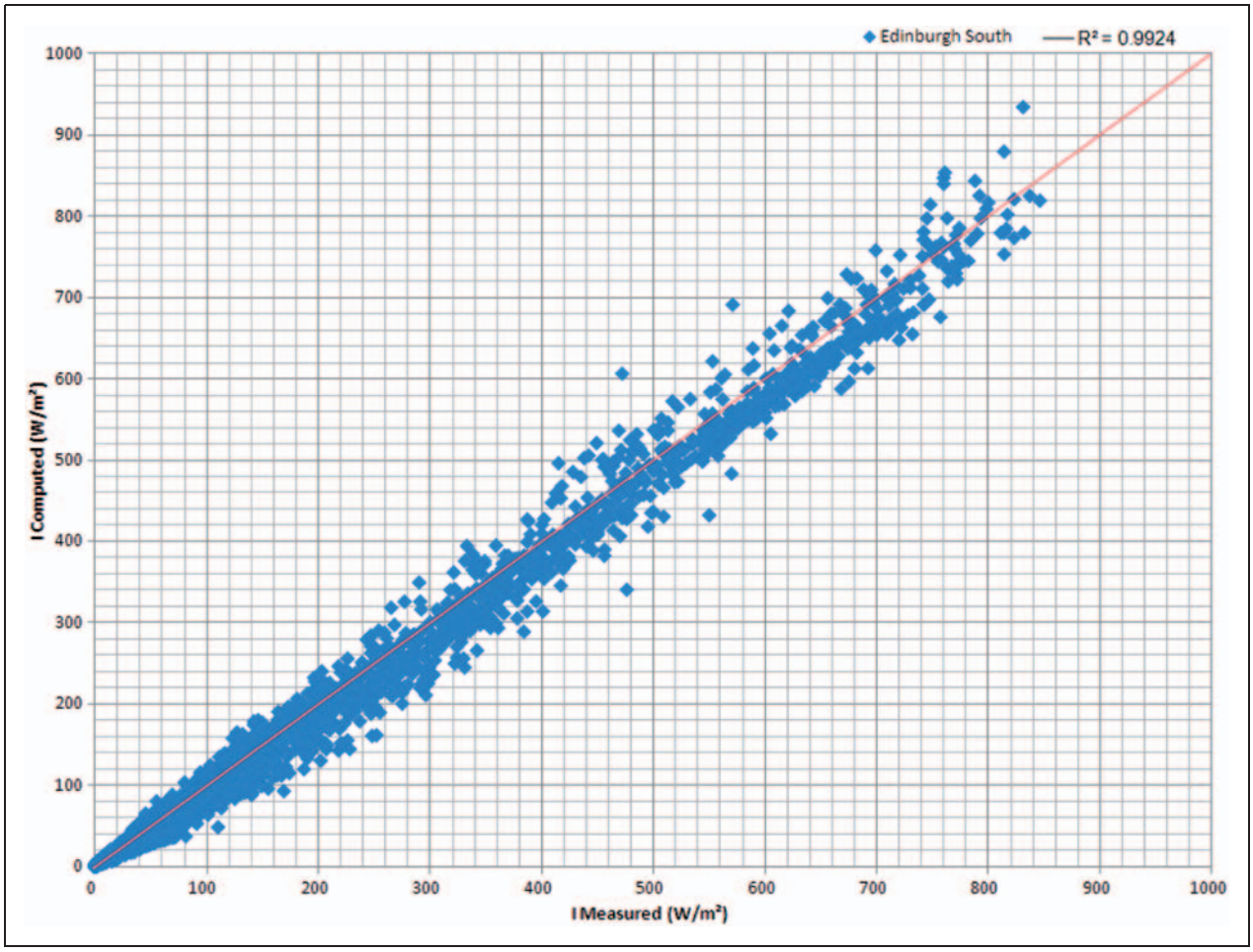

Figure 9. Hourly computed vs experimental slope irradiance for Edinburgh – South aspect.

equation (19) with "Δx" the width of component in meters and "k" the thermal conductivity of the corresponding material expressed in (W/m K).

$$R = \frac{\Delta x}{k} \tag{19}$$

The mass measured and specific heat capacities of each material composing the solar house are shown in Table 2.[21,22] Total internal and external thermal mass "$\sum m \times C_{P_{is}}$" and "$\sum m \times C_{P_{os}}$" required for the analysis Q_{loss} were calculated.

Referring back to Figure 15, the dynamic thermal model has three capacitance nodes: outside, outer and inner surface. During the day, T_{is} increases because it receives energy from the sun and decreases during the night due to a large heat loss from windows and the roof (large view factor to sky). On clear nights, the sky acts as a nearly perfect receiver of the thermal radiation. T_i increases during the day and decreases during the night.[22]

Determination of energy loss (Q_{loss1}, Q_{loss2} and Q_{loss3})[22]

Q_{loss1} = Heat loss by windows in (W) is defined by Equation (20):

$$Q_{loss1} = U_{windows} \times A \times (T_{is} - T_o) \tag{20}$$

where $U \times A$ value is taken from Table 3. A represents the surface area of the corresponding component of the building expressed in (m^2).

$Q_{loss2} = Q_{in2}$ = Heat loss by walls in (W) is defined by equation (21):

$$Q_{loss2} = \sum U \times A \times (T_{is} - T_{os}) \tag{21}$$

where "$\sum U \times A$" value is taken from Table 4. Q_{loss3} = Heat loss of outside surfaces in (W) is defined by equation (22):

$$Q_{loss3} = \sum h \times A \times (T_{os} - T_o) \tag{22}$$

where "$\sum h \times A$" is taken from Table 5.

Figure 10. Solar house built with structural insulated panels (SIPs).

Inner skin temperature calculation layout

Referring to the PSSH model – spreadsheet, at time = 0 s, the heat exchange between the air and the inner surface is assumed to be zero in a constant and stabilised scheme. Thus, the temperature inside the building, taken from the measurements, was considered equal to the inner surface temperature of the solar house: $T_i = T_{is}$ at $t = 0$ s

From this assumption, Q_{loss1} was calculated using equation (23):

$$Q_{loss1} = U_{windows} \times A \times (T_{is} - T_o) \tag{23}$$

Then, to calculate Q_{loss2}, the outer skin temperature "T_{os}" was required to determine the temperature difference ($T_{is} - T_{os} = ?$) needed for the calculation of losses by walls. At $t = 0$s, the outer skin temperature "T_{os}" was considered constant, which means the energy lost by convection by walls "Q_{loss3}" is assumed equal to the energy gained by conduction of the wall "Q_{in2}".

At $t = 0$ second, the energy equation can be written as follows:

$$Q_{loss2(wall)} = Q_{in2(wall)} = Q_{loss3(convection\ wall)}$$

This assumption is developed as represented by equation (24) as:

$$\sum U \times A \times (T_{is,\,t=0s} - T_{os,t-0s}) = \sum h \times A \times (T_{os,t=0s} - T_{o,t-0s}) \tag{24}$$

and "T_{os}" is obtained from equation (25):

$$T_{os,t=0s} = \frac{\sum U \times A \times T_{is,t=0s} + \sum h \times A \times T_{o,t=0s}}{\sum h \times A + \sum U \times A} \tag{25}$$

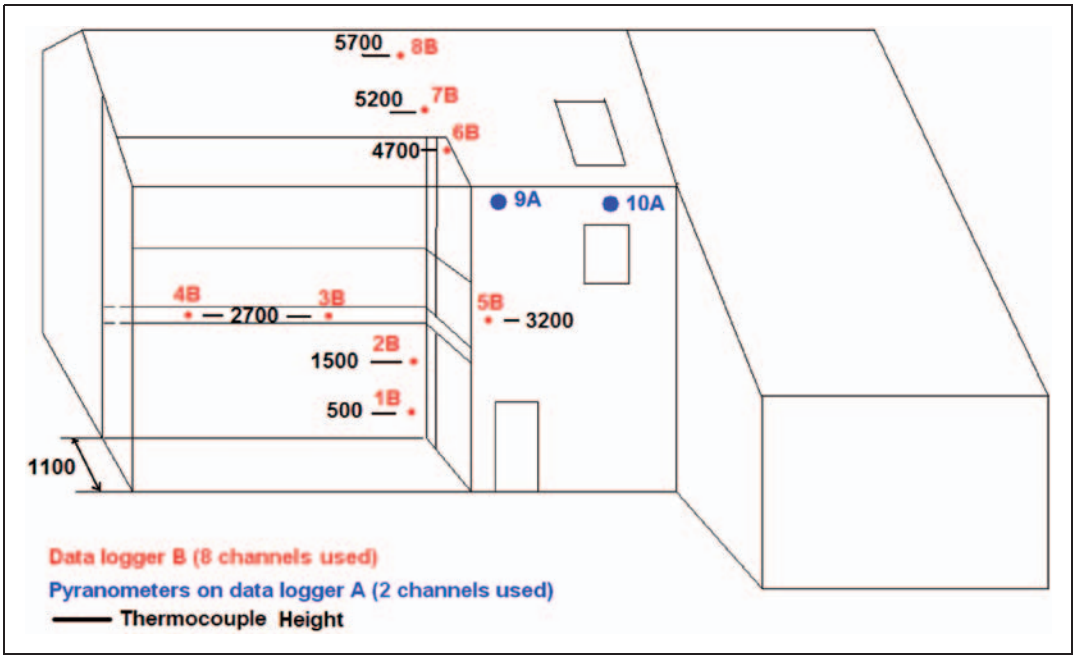

Figure 11. Description of the solar house and location of the measurement devices.

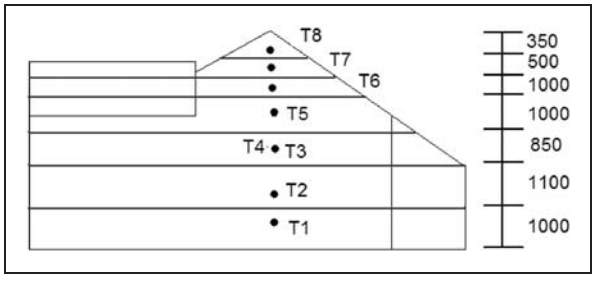

Figure 12. Control volume approach for weighted average temperature of air.

Now "Q_{loss2}" and "Q_{loss3}" are calculated from Equation (26) and (27) respectively:

$$Q_{loss2} = Q_{in2} = \sum U \times A \times (T_{is,t=0s} - T_{os,t=0s}) \quad (26)$$

and

$$Q_{loss3} = \sum h \times A \times (T_{os,t=0s} - T_{o,t=0s}) \quad (27)$$

On the PSSH model – spreadsheet, the measurement after 10 min ($t = 600$ s), the inner and outer skin temperatures were assumed to be the same as the one taken 600 s before that the reason why, (Q_{loss1}, Q_{loss2} and Q_{loss3}) were calculated from "T_{is}" and "T_{os}" the row below as shown in equations (28–30), 600 s before.

$$Q_{loss1} = U \times A \times (T_{is,t=0s} - T_{o,t=600s}) \quad (28)$$

$$Q_{loss2} = \sum U \times A \times (T_{is,t=0s} - T_{os,t=0s}) \quad (29)$$

$$Q_{loss3} = \sum h \times A \times (T_{os,t=0s} - T_{o,t=600s}) \quad (30)$$

Then inner and outer skin temperatures were calculated by the transient thermal analysis named the "Lumped Capacitance" method.

As demonstrated before, the solar house can be considered a 1 mass element. This mass has a thermal density equal to $m \times C_P$ (Equation (31)):

$$m \times C_{P_{is}} \times \frac{\Delta T_{is}}{dt} = m \times C_{P_{is}} \times \frac{T_{is,t=600s} - T_{is,t=0s}}{600} = Q_{in} - Q_{loss1} - Q_{loss2} \quad (31)$$

ΔT_{is}, is the inner skin temperature difference in 10 min and is defined by equation (32) as:

$$\Delta T_{is} = \frac{Q_{in} - Q_{loss1} - Q_{loss2}}{\sum m \times C_{P_{IS}}} \times 600 \quad (32)$$

Using equation (33):

$$\sum m \times C_{P_{is}} = m \times C_{P_{walls}} + m \times C_{P_{windows}} \quad (33)$$

Then, the new inner skin temperature was obtained using equation (34):

$$T_{is,t=600s} = T_{is,t=0s} + \Delta T_{is} \quad (34)$$

Now, to find the new "T_{os}", the "ΔT_{os}" needs to be calculated by using equation (35) of the same Lumped

Table 1. Thermal characteristics of the house.

Component	Area m^2	*U* Values $W\ m^{-2}\ K$	h^{15} $W\ m^{-2}\ K$	UA $W\ K^{-1}$	Component's location
Roof	98.42	0.22	25	21.65	
Sloping roof	43.17	0.35	16.7	15.11	200 mm insulation
Partition walls		2.1	16.7	0	Kitchen/Bedr Internal Wall
External walls	166.53	0.4	16.7	66.61	
Windows	47.06	3.3	16.7	155.3	
Windows	0	6	16.7	0	Wood DG
Doors	5.88	3.3	16.7	19.4	Single glazed Normal
Ground floor	128.78	0.25	25	32.19	150 mm insulation
Ceiling/floor	83.63	0	16.7	0	
Total area = 573.46 m^2			$\sum UA = 310.27\ W/K$		

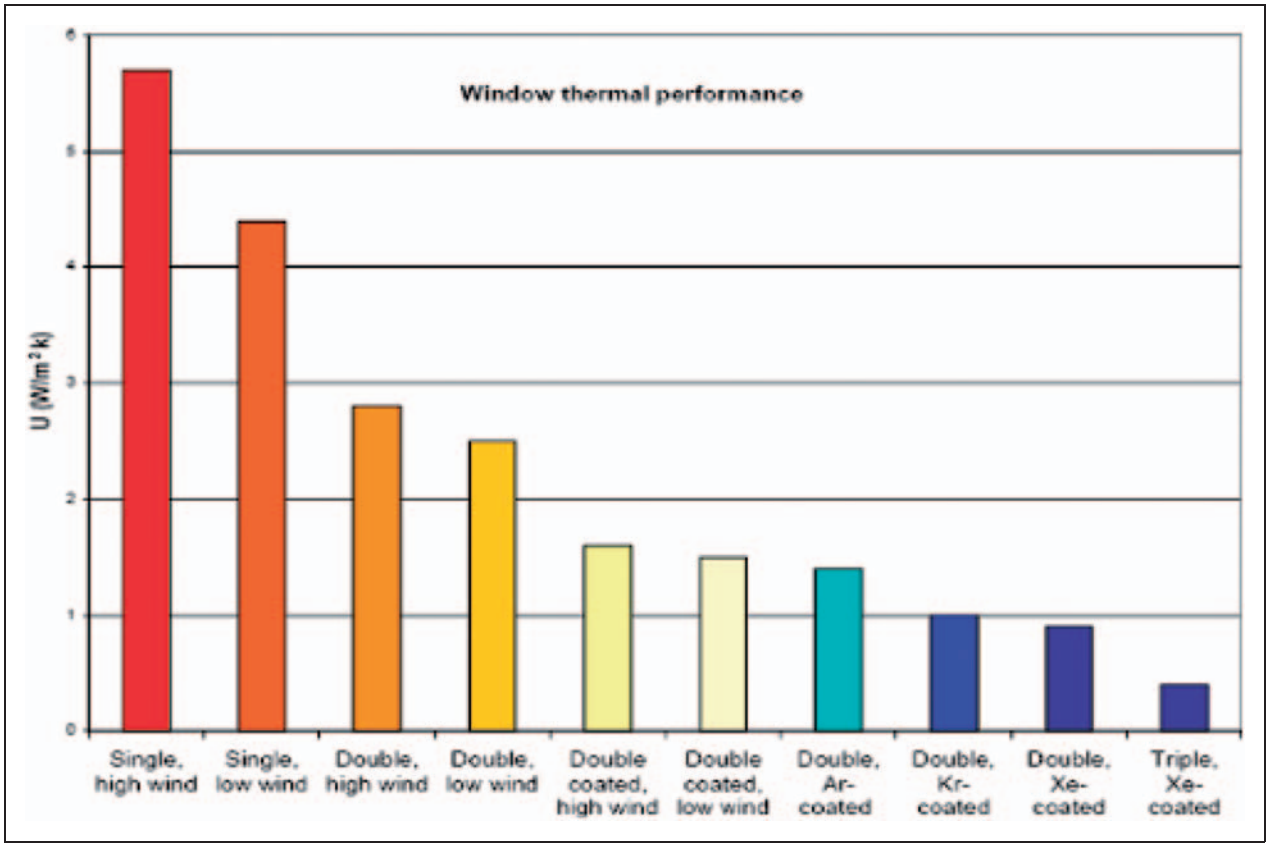

Figure 13. Evolution of super-insulated windows – by the introduction of inert gases and low-emissive glass coating, the heat loss has been reduced by a factor of 14.

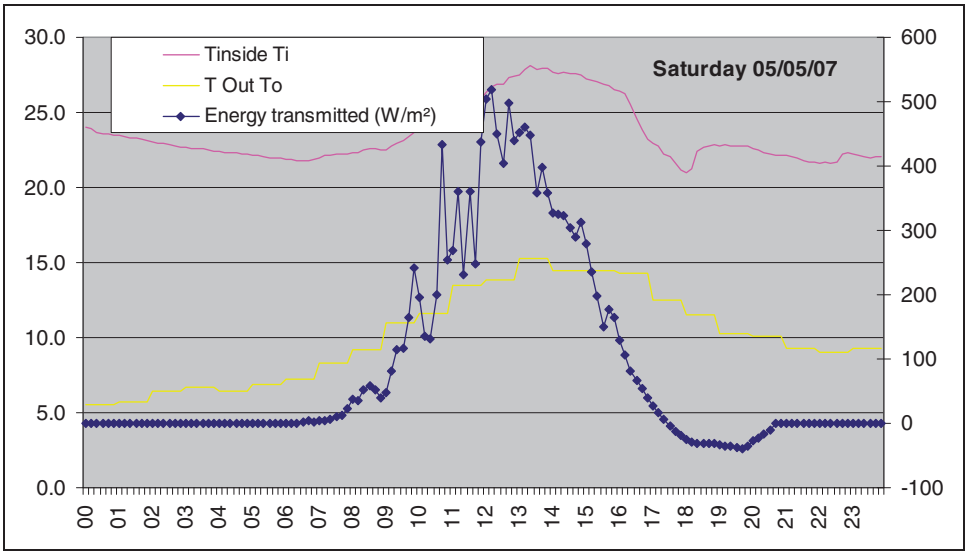

Figure 14. Inner and outer average temperature with the solar radiance profile.

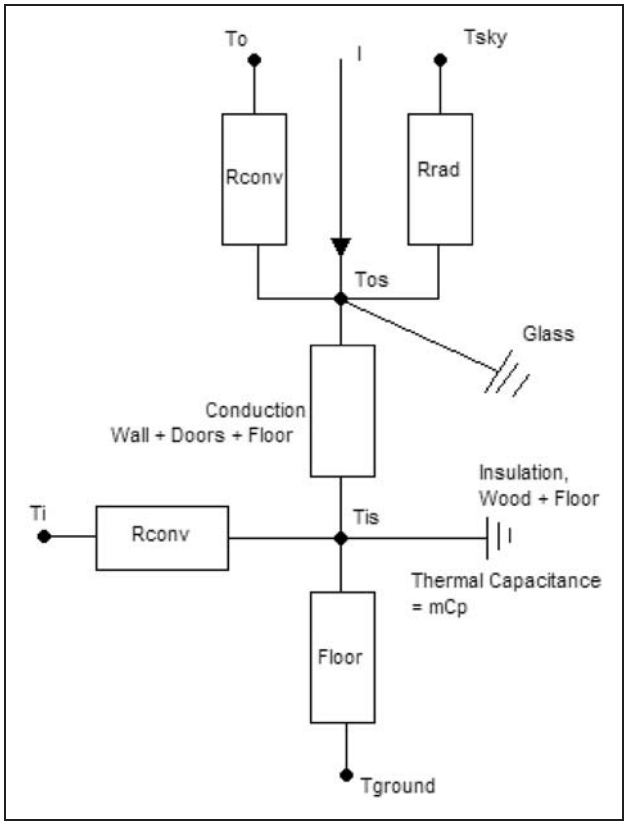

Figure 15. Thermal resistance network for the solar house.

capacitance method:

$$\sum m \times C_{P_{os}} \times \frac{\Delta T_{os}}{dt} = \sum m \times C_{P_{os}} \times \frac{T_{os,t=600s} - T_{os,\,t=0s}}{600} = Q_{in2} - Q_{loss3} \tag{35}$$

The inner skin temperature difference "ΔT_{os}" in 10 minutes is defined by equation (36) as:

$$\Delta T_{os} = \frac{Q_{in2} - Q_{loss3}}{\sum m \times C_{P_{os}}} \times 600 \tag{36}$$

Using the new energy gained "Q_{in2}" was calculated from equation (37):

$$Q_{in2} = \sum U \times A \times (T_{is,t=600s} - T_{os,t=0s}) \tag{37}$$

Then, from Equation (38)

$$\sum m \times C_{P_{os}} = m \times C_{P_{wall}} \tag{38}$$

Simulation result and analysis

Once the above analysis was simulated on a spreadsheet application, the computer-generated inner skin temperatures were obtained. The results were plotted and

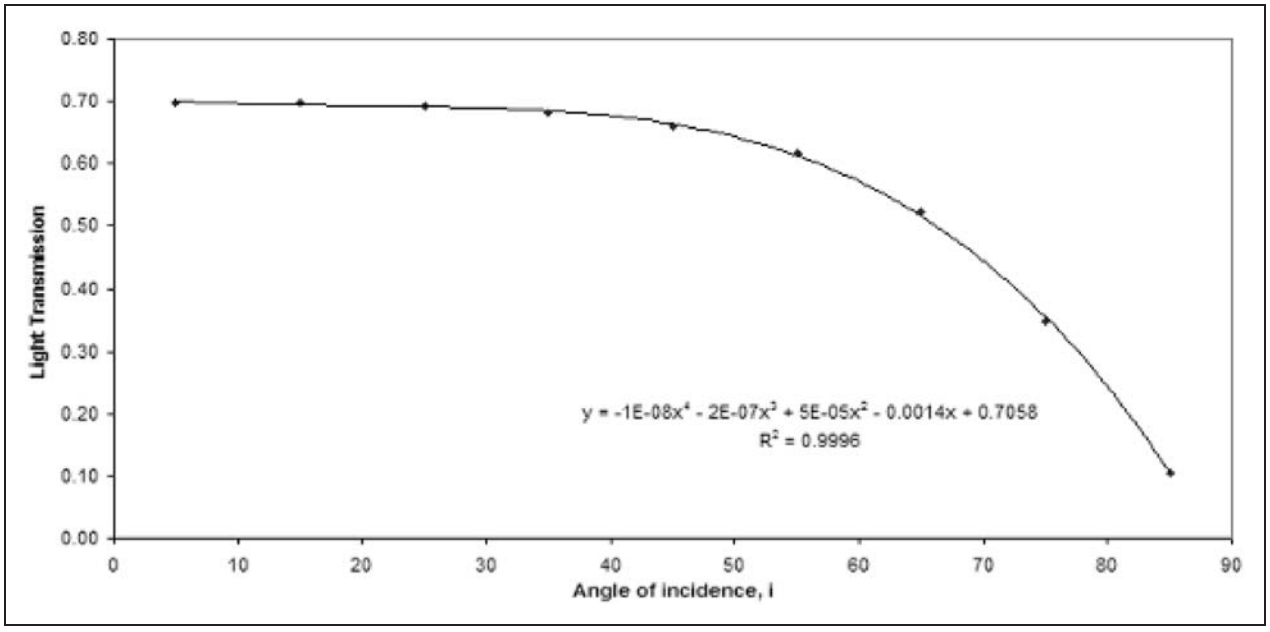

Figure 16. Transmission curve for the double-glazed window (6 mm thickness).

can be seen in Figure 18. The simulated temperatures profile of "T_{is}" and "T_{os}" have a similar shape than the measured inner and outer temperatures "T_i" and "T_o" of the solar house.

Comparison between the simulated inner skin temperature and monitored internal temperature

The simulated outer skin temperature profile was the same as the outer temperature profile measured. The software works very well for the outer skin temperature simulation but can have uncertainty for the inner skin temperature model. The simulated inner skin temperature profile follows the inner temperature measured but a temperature difference still remains.

The difference can be explained due to the infiltration rate not taken into account. The technique applied can be improved by simulating more nodes in the thermal network to obtain more accurate results. Another way to decrease the temperature difference between "T_i" and "T_{is}" would be to simulate more accurately the building envelope thermal characteristics and input more internal thermal mass details. Indeed, by changing the value of the thermal mass, the thermal conductivity, the U Value, the density, the heat losses vary with the temperature profile.

Comparison using TAS and IES modelling software

The PSSH simulation software was compared with two successive simulations via integrated environmental solution (IES) and thermal analysis simulation (TAS) in order to evaluate the accuracy.

TAS and IES software are used predominantly in the British building services sector. TAS is a suite of software products, which simulate the dynamic thermal performance of buildings and their systems. The main module is TAS Building Designer, which performs dynamic building simulation with integrated natural and forced airflow. It has 3D graphics-based geometry input that includes a CAD link. It allows design professionals to compare alternative heating/cooling strategies and façade design for comfort, equipment sizing and energy demand.[23] Capable of performing dynamic thermal simulation for all type of buildings, TAS allows designers to accurately predict energy consumption, CO_2 emissions, operating costs and occupant comfort.[24]

Integrated Environmental Solution – Virtual Environment (IES-VE) consists of a suite of integrated analysis tools, which can be used to investigate the performance of a building either retrospectively or during the design stages of a construction project. A model of a building can be constructed using the "ModelIT" module, which can then be analysed in a variety of ways. Most commonly used is the "Apache" thermal analysis module, which provides either steady-state or dynamic analysis of energy consumption and indoor thermal conditions.[25]

The data inputted in TAS and IES were, respectively, the same as the one used in the PSSH simulation. The weather data used in TAS and IES simulations are the CIBSE sub-hourly weather data from Edinburgh airport. A comparison of the PSSH simulation software

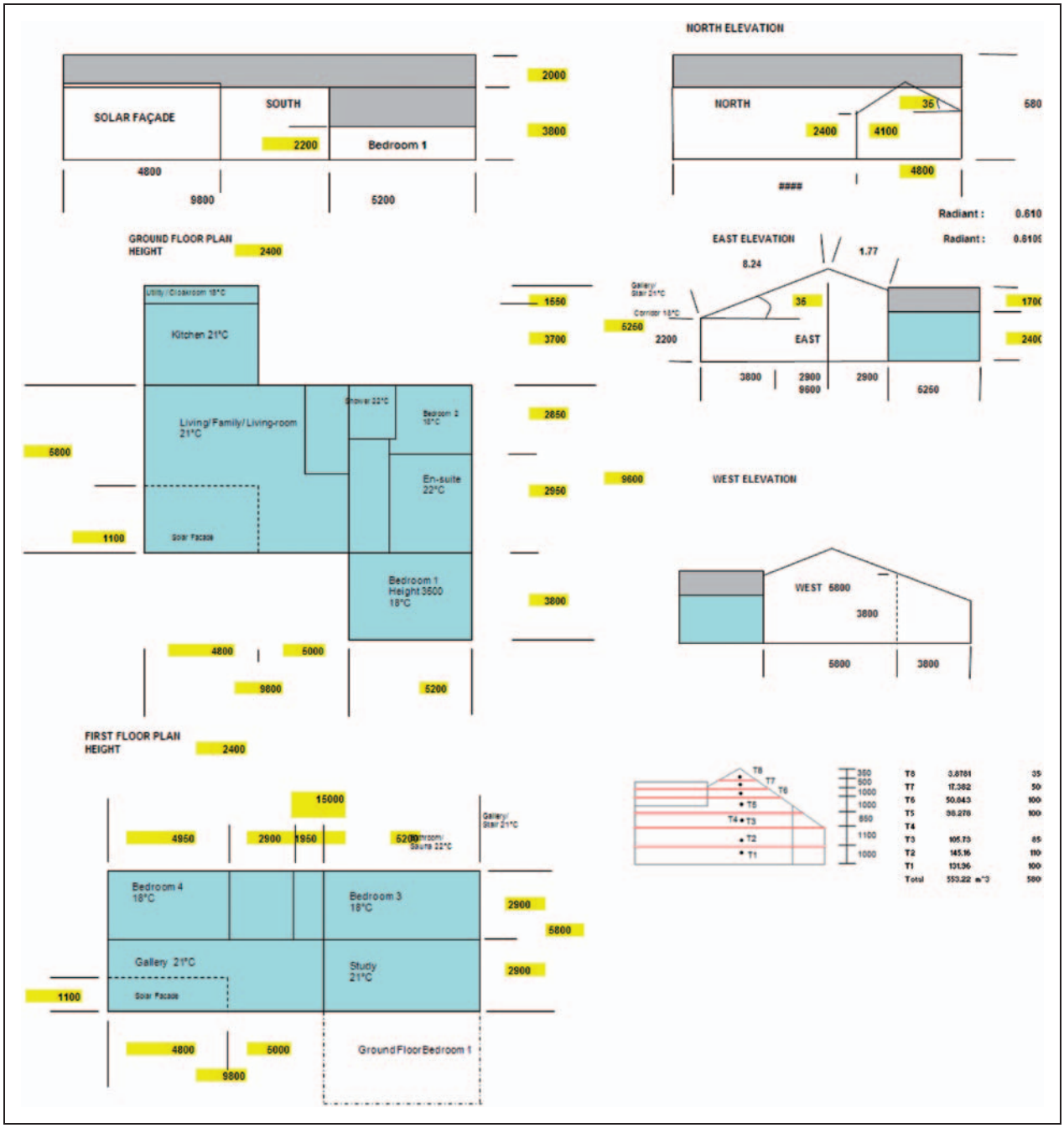

Figure 17. Solar house architectural detail.

Table 2. Thermal mass calculation of the building.[19,20]

Building material	Width (m)	Volume (m^3)	Density ($kg\,m^{-3}$)	Mass (kg)	C_p ($J/kg\,K$)	mC_p ($J\,K^{-1}$)
Glass	0.003	0.14	2600	367	880	3.2E + 05
Inner OSB sheathing	0.011	5.73	545	3120	1220	3.8E + 06
Polyurethane foam	0.103	53.61	16	858	840	7.2E + 05
Outer OSB sheathing	0.011	5.73	255	1460	1380	2.0E + 06
Plasterboard	0.012	5.07	256	1297	1380	1.8E + 06
Concrete block	0.012	5.07	257	1302	1380	1.8E + 06
Roof slates	0.012	0	258	0	1380	0.0E + 00
$\sum m \times C_{P_{is}}$						2.6E + 07
$\sum m \times C_{P_{os}}$						6.5E + 06

Table 3. UA calculation for Q_{loss1}.

For Q_{loss1}: Windows	
h windows ($W\,m^{-2}\,K$)	16.7
U windows ($W\,m^{-2}\,K$)	3.3
$U = 1/(1/h + 1/U)$ ($W\,m^{-2}\,K$)	2.76
UA (W/K)	129.67

Table 4. UA calculation for Q_{loss2} and Q_{in2}.

For Q_{loss2} and Q_{in2}: Loss Wall	U ($W\,m^{-2}\,K$)
Walls without floor	0.4
Roof 79′	0.22
Door	3.3
Floor	0
ΣUA (W/K)	107.67

Table 5. UA calculation for Q_{loss3}.

For Q_{loss3}: Outside surfaces	h ($W\,m^{-2}\,K$)
Walls + windows	16.7
Roof	25
ΣhA (W/K)	7938.67

was performed with the commercially available simulation software IES.

It was demonstrated that this model has an influential impact on the determination of the use of passive solar space heating as LZCES. In the present work, PSSH model was tested. Results were compared with TAS and IES simulation software (Figure 19). The results show that simulated inner temperatures "T_i" from IES and TAS are less accurate but the analysis needs to consider the different methods of calculations and the weather data used in relation to the location. It is difficult to draw a final conclusion on the results found as the IES and TAS software do not allow the use of the temperature for a specific location, where PSSH model does.

Conclusion

It has been shown with this study that passive solar energy can have significant influence on the building internal temperature. As a renewable energy, this technology can considerably improve the building energy efficiency and reduce its carbon emissions. Passive solar space heating can be considered as an LZCES.

This building thermal model introduced in this work was proven to have an influential impact on the determination of onsite solar energy available in

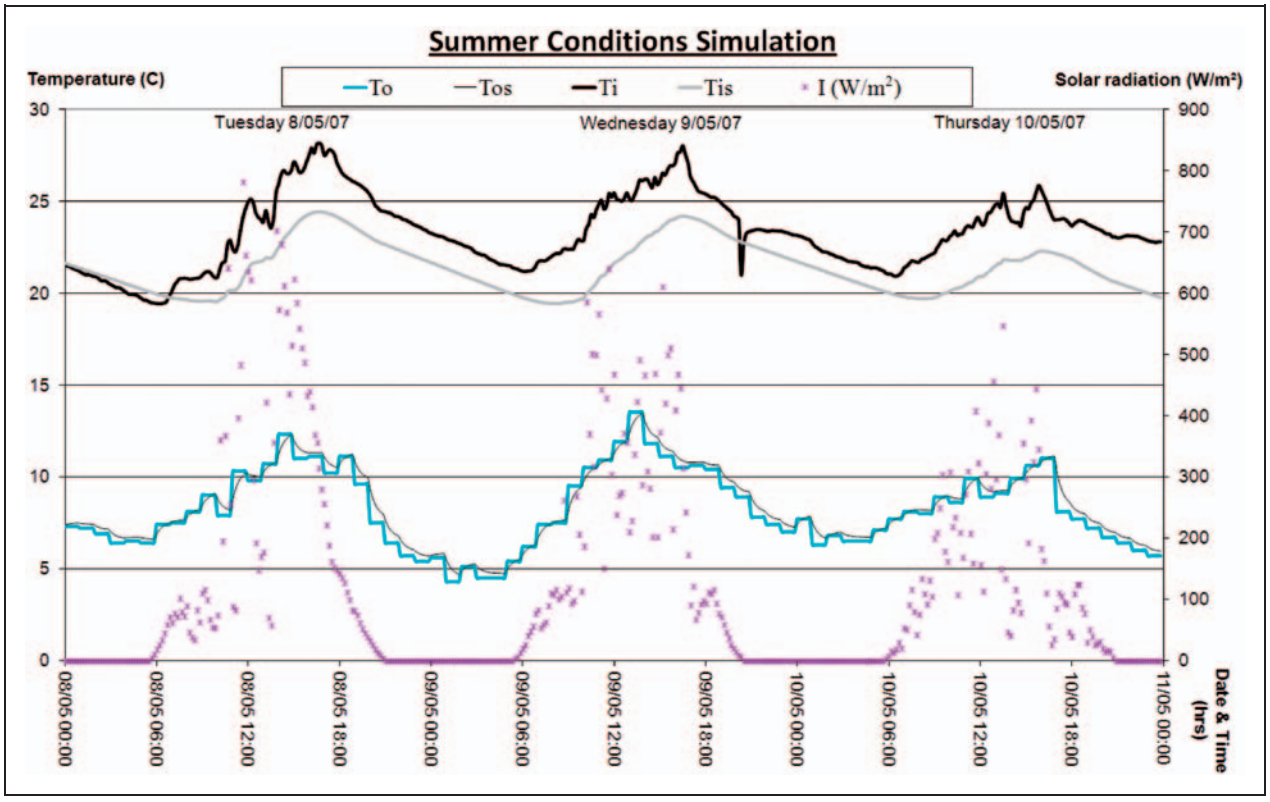

Figure 18. Summer experimental and simulation of inner and outer skin temperature (T_{is} and T_{os}).

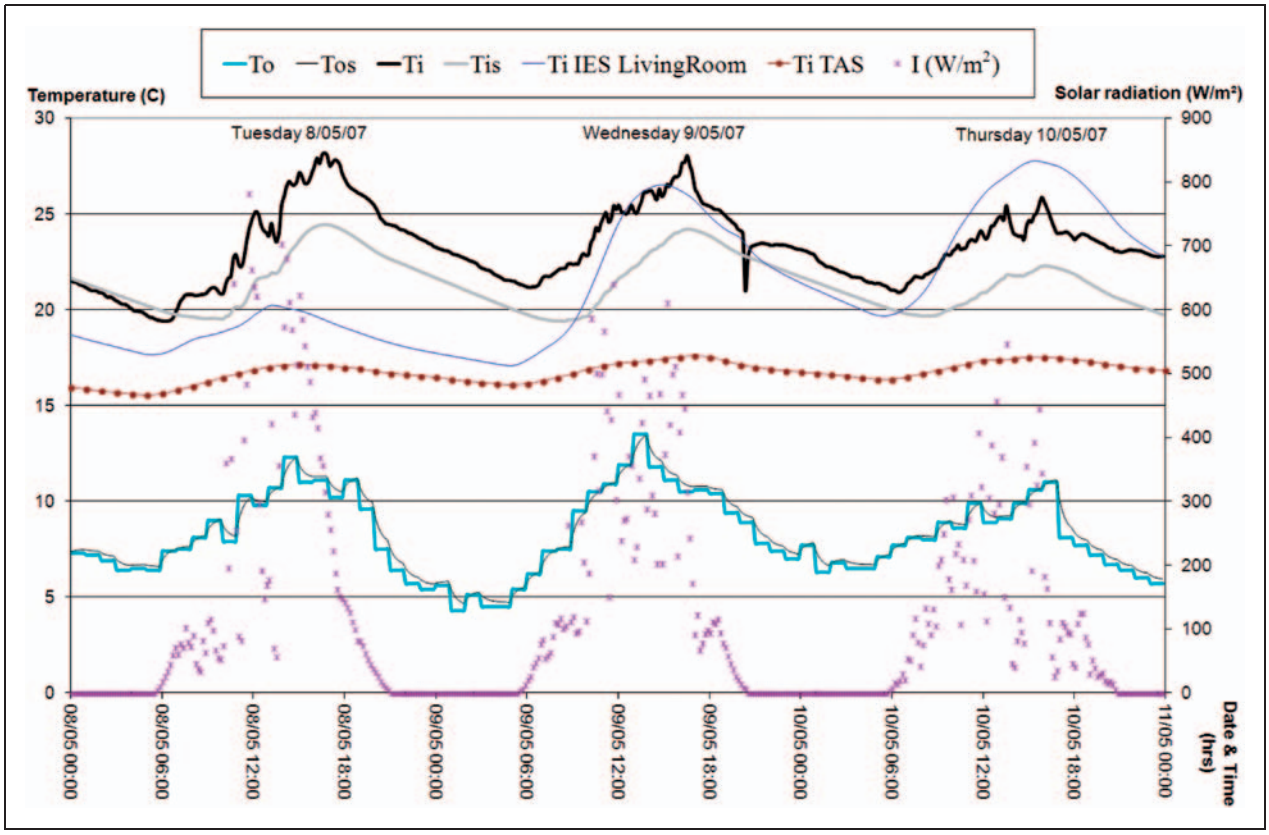

Figure 19. Comparison between inner temperatures (T_i) obtained from IES, TAS and PSSH model.
IES: integrated environmental solution; TAS: thermal analysis simulation.

UK conditions. This tool can be used by building services engineers as a decision-making tool to design buildings that satisfy the government Regulations.

Such proposals towards the direction of evaluating the solar space heating potential can be adopted in the building services sector given the appropriate incentives by funding and legislation.

To conclude, the solar space heating simulation tool takes less time to model and allows more flexibility than other software packages which are very time consuming.

Acknowledgements

Thanks to Mr and Mrs Finch for kindly letting us to monitor their solar house in East Whitburn, Scotland. The illuminance meters and dataloggers were provided by Napier University with assistance from Ian Campbell and Kevin McCann measurements and other data collection. The assistance of all the above is gratefully acknowledged.

References

1. Li DHW, Yang L and Lam JC. Impact of climate change on energy use in the built environment in different climate zones – A review. *Energy* 2012; 42(1): 103–112.
2. Levermore GJ. A review of the IPCC assessment report four, part 1: the IPCC process and greenhouse gas emission trends from buildings worldwide. *Build Serv Eng Res Technol* 2008; 29: 349–361.
3. Office of the Deputy Prime Minister. Conservation of Fuel and Power in new dwellings. Approved document, *Part L1A*, ODPM, The Building Regulations, London, 2010.
4. Office of the Deputy Prime Minister. Conservation of Fuel and Power in existing dwellings. Approved document, *Part L1B*, ODPM, The Building Regulations, London, 2010.
5. Office of the Deputy Prime Minister. Conservation of Fuel and Power in new buildings other than dwellings. Approved document, *Part L2A*, ODPM, The Building Regulations, London, 2010.
6. Office of the Deputy Prime Minister. Conservation of Fuel and Power in existing buildings other than dwellings. Approved document, *Part L2B*, ODPM, The Building Regulations, London, 2010.
7. Sartori I, Napolitano A and Vossc K. Net zero energy buildings: A consistent definition framework. *Building Environ* 2012; 48: 220–232.
8. Yu CWF and Kim JT. Low carbon housings and indoor air quality. *Indoor Built Environ* 2012; 21(1): 5–15.
9. Boyle G. *Renewable Energy, Power for a Sustainable Future*. 1st ed. Oxford: Oxford University Press, 1996.
10. Chesné L, Duforestel T, Roux JJ, et al. Energy saving and environmental resources potentials: Toward new methods of building design. *Building Environ* 2012; 58: 199–207.
11. Office of the Deputy Prime Minister. Low or Zero Carbon Energy Sources: Strategic Guide, The Building Regulations 2000, ODPM, London, 2006.

12. The Chartered Institute of Building Services Engineers, CIBSE. Test Reference Years (TRYs) and Design Summer Years (DSYs) Hourly Weather Data Set (14 sites). London, CIBSE, 2006.
13. The Chartered Institute of Building Services Engineers. CIBSE Guide C: Reference Data. CIBSE Knowledge Portal, London, 2007 (ISBN: 9781903287804).
14. Kopp G and Lean JL. A new, lower value of total solar irradiance: Evidence and climate significance. *Geophys Res Lett* 2011; 38: L01706.
15. Muneer T. *Solar Radiation and Daylight Models*. Oxford: Butterworth-Heinemann, 2004.
16. Duffie JA and Beckman WA. *Solar Energy Thermal Processes*. New York: John Wiley and Sons, 1974.
17. Muneer T. *Windows in Buildings: Thermal, Acoustic, Visual & Solar Performance*. Oxford: Architectural Press, 2000.
18. Kreider JF and Kreith F. *Solar Energy Handbook*. New York: Mcgraw-Hill Book Company, 1981.
19. Woolf HM. On the Computation of Solar Evaluation Angles and the Determination of Sunrise and Sunset Times. Houston, National Aeronautics and Space Administration Report, NASA, 1968.
20. Muneer T, Maubleu S and Asif M. Prospects of solar water heating for textile industry in Pakistan. *Renew Sustainable Energy Rev* 2006; 10(1): 1–23.
21. The Chartered Institute of Building Services Engineers. CIBSE Guide A: Environmental Design, 7th edn. London, CISBE, 2007.
22. Muneer T, Kubie J and Grassie T. *Heat Transfer, a Problem Solving Approach*. London: Taylor and Francis, 2003.
23. GREEN BIM blog. Green Design with Building Information Modeling and analysis tools, www.greenbim.blogspot.com.es/2007/07/tas-building-simulation-software.html (accessed January 24, 2013).
24. Environmental Design Solutions Limited. TAS software, www.edsl.net/main/Software.aspx (accessed January 24, 2013).
25. University of Cambridge. Energy modelling and building physics resource base, www-embp.eng.cam.ac.uk/software/iesve (accessed January 24, 2013).